Journal of Catalysis 258 (2008) 243–249

Contents lists available at ScienceDirect

Journal of Catalysis

www.elsevier.com/locate/jcat

Selective production of propylene from methanol: Mesoporosity development in high silica HZSM-5

Changsong Mei [a,c,1], Pengyu Wen [b,1], Zhicheng Liu [a], Hongxing Liu [a], Yangdong Wang [a], Weimin Yang [a], Zaiku Xie [a,*], Weiming Hua [c,*], Zi Gao [c]

[a] Shanghai Research Institute of Petrochemical Technology, SINOPEC, 1658 PuDong Beilu, Shanghai 201208, PR China
[b] School of Chemistry and Molecular Engineering, East China University of Science and Technology, Shanghai 200237, PR China
[c] Department of Chemistry and Shanghai Key Laboratory of Molecular Catalysis and Innovative Materials, Fudan University, Shanghai 200433, PR China

ARTICLE INFO

Article history:
Received 14 April 2008
Revised 13 June 2008
Accepted 15 June 2008
Available online 17 July 2008

Keywords:
HZSM-5
Methanol-to-propylene process
Propylene selectivity
Propylene/ethylene ratio
Mesoporosity
Diffusion

ABSTRACT

The mesoporosity development in high silica HZSM-5 was carried out by alkaline desilication treatment and soft template method, and its relationship with the catalytic performance of the modified catalysts in methanol-to-propylene reaction was studied. High propylene selectivity (42.2%) and propylene/ethylene ratio (10.1) were observed on the high silica HZSM-5 catalyst modified by alkaline desilication. The enhanced catalytic performance can be attributed to the newly created open mesopores on the surface of the zeolite crystals together with the low Brønsted acidity. A greater amount of mesoporosity could be readily formed in HZSM-5 crystals via the soft template route. However, the mesopores formed in this method are randomly distributed in the zeolite crystals and play a minor role in the molecular transport of the reaction, so the improvement in propylene selectivity and propylene/ethylene ratio of the catalyst is less evident. The higher propylene selectivity and propylene/ethylene ratio on modified HZSM-5 (especially by alkaline treatment) than unmodified HZSM-5 could be also related to different contributions of the methylaromatics route and olefins methylation/cracking route in MTP reaction.

1. Introduction

Propylene is one of the most important commodity petrochemicals, as a raw material for the production of polypropylene, polyacrylonitrile, acrolein and acrylic acid. Nowadays, propylene is mainly produced as a by-product of petroleum refining and of ethylene production by the naphtha steam-cracking process. Due to the growing demand for propylene and the shortage of petroleum resource in the future, new processes with high-yield of propylene are required. Methanol-to-olefins (MTO) and methanol-to-propylene (MTP) processes are promising alternative ways for the production of propylene instead of petroleum route, since methanol can be easily produced from natural gas and coal. So, these two new routes have attracted significant attention [1–3]. As compared to the traditional MTO process, where ethylene is the main product, high propylene to ethylene (P/E) ratio is the most distinguishable feature for MTP process that enables the high propylene yield in the recirculation process.

Much attention has been paid to MTO process employing zeolite catalysts [1,2,4–7]. So far, there are few reports concerning MTP process [3,8]. One-pass selectivity to propylene and P/E ratio are still low in the current researches on MTP reaction [8,9], while high P/E ratio is vital to producing propylene from methanol employing recycling technics [8,10]. High P/E ratio can be achieved under the condition of low methanol partial pressure resulted from use of excessive carrier gas or feed with high water/methanol ratio. However, too low methanol partial pressure is uneconomic from the practical point of view. Chang et al. reported that decreasing Brønsted acidity of HZSM-5 zeolite could improve its selectivity to propylene in MTO reaction [11]. Prinz and Riekert observed that the selectivity for formation of ethylene and propylene as well as P/E ratio increased with decreasing HZSM-5 crystal size during the catalytic conversion of methanol to hydrocarbons [12], indicating that shortening of the diffusion path in HZSM-5 zeolite may increase the P/E ratio.

In the present work, two kinds of mesopore-modified high silica HZSM-5 zeolites were prepared by alkaline treatment and soft template method. These samples were well characterized by various methods and used in MTP reaction. Our main purpose is to get a better insight into the influence of mesoporosity development on diffusion and catalytic performance of the zeolite catalysts in MTP reaction through comparison of the structural and catalytic properties of samples obtained by different modification methods.

* Corresponding authors. Faxes: +86 21 68462283 (Z. Xie), +86 21 65641740 (W. Hua).
E-mail addresses: xiezk@mail.sript.com.cn (Z. Xie), wmhua@fudan.edu.cn (W. Hua).
[1] Changsong Mei and Pengyu Wen contributed equally to this work.

0021-9517/$ – see front matter
doi:10.1016/j.jcat.2008.06.019

2. Experimental

2.1. Catalyst preparation

Parent ZSM-5 zeolites with different Si/Al molar ratios were synthesized hydrothermally from the corresponding aluminosilicate gels. Tetrapropylammonium hydroxide (TPAOH) was used as the template. The silicon source was colloidal silica, and the aluminum source was $NaAlO_2$. Both colloidal silica and $NaAlO_2$ were from Sinopharm Chemical Reagent Co., Ltd. The molar composition of the synthesis mixture was $xSiO_2$:$1Al_2O_3$:8TPAOH:$800H_2O$, where x was 20, 80, 140 and 220. After being stirred for 7 h at 25 °C, the gel was transferred into an autoclave and crystallized at 180 °C for 5 days. The product was filtered, washed, dried at 110 °C overnight and then calcined at 550 °C for 5 h to remove the template. The parent ZSM-5 zeolites were turned into the H-form by three consecutive ion exchanges in 1 M HCl solution with a solution/zeolite ratio of 10 cm^3/g at 90 °C for 9 h. The obtained HZSM-5 samples were labeled as S1, S2, S3 and S4, of which the Si/Al molar ratio of the starting gel was 10, 40, 70 and 110, respectively. The S3 sample was subjected to mesoporosity generation by alkaline treatment in 0.45 M Na_2CO_3 solution with a solution/zeolite ratio of 15 cm^3/g at 75 °C for 30 h [13–17]. The obtained product was then filtered, washed, dried and then exchanged in 1 M HCl solution for three times with a solution/zeolite ratio of 10 cm^3/g at 90 °C for 9 h to get the final mesopore-modified HZSM-5 which was designated as S5. For comparison, another kind of mesoporous HZSM-5 with Si/Al molar ratio of 76 (labeled as S6) was synthesized by the soft template route. Synthesis of S6 was in the same way as S3, except that 5 wt% starch was added into the gel with molar composition of $140SiO_2$:$1Al_2O_3$:8TPAOH:$800H_2O$.

2.2. Catalyst characterization

X-ray powder diffraction (XRD) patterns were recorded on a Rigaku D/max-1400 diffractometer with Ni-filtered Cu$K\alpha$ radiation operated at 40 kV and 100 mA. The relative crystallinity of the sample was determined by measuring the intensity of its peaks at $d = 3.851$, 3.823, 3.798, 3.732 and 3.711 nm and comparing the sum of the intensities with that of the reference sample S3. The N_2 adsorption/desorption isotherms of the samples were measured by using a Micromeritics TriStar 3000 system at liquid-N_2 temperature. The Brunauer–Emmett–Teller (BET) surface area was calculated from the adsorption isotherm, and the mesopore size distribution was derived from the adsorption isotherm according to the BJH model. The surface morphology and crystallite size of the samples were determined by scanning electron microscopy (SEM) recorded on a JEOL JSM-35C microscope. Transmission electron microscopy (TEM) was recorded on a JEM-CX-II instrument. The samples were prepared by dispersing the powder products as a slurry in ethanol, which was then deposited and dried on a holey carbon film on a Cu grid. ^{27}Al magic-angle spinning nuclear magnetic resonance (MAS NMR) spectra were recorded on a Varian 400 spectrometer. A resonance frequency of 101.19 MHz, a recycle delay of 0.6 s, pulse widths of 0.4 μs and a spinning rate of 5 kHz were applied. ^{27}Al chemical shifts were reported relative to $Al(H_2O)_6^{3+}$. The NMR analysis was carried out with the samples prehydrated in a wet desiccator for several days. The acidic properties (Brønsted and Lewis acid sites) of the samples were investigated by Fourier transform infrared (FTIR) spectra of adsorbed pyridine in an in situ cell with CaF_2 windows. Self-supporting wafers of the samples were pretreated at 400 °C for 2 h under 10^{-2} Pa and then cooled to 200 °C. After the pyridine adsorption at 200 °C for 15 min and evacuation at 200 °C for 30 min, IR spectra were recorded on a Bruker IFS 88 spectrometer with a resolution of 4.0 cm^{-1}. Brønsted and Lewis acidities were quantified with the integrated areas of the absorbance peaks at 1540 and at 1450 cm^{-1}, respectively. The bulk Si/Al molar ratios of the samples were determined by inductively coupled plasma (ICP) spectroscopy.

2.3. Catalytic test

The MTP reaction was carried out at 470 °C in a flow-type fixed-bed microreactor under atmospheric pressure. The catalyst load was 3 g and the weight hourly space velocity (WHSV) for methanol was 1 h^{-1}. Water vapor was used as diluent and the partial pressure of methanol was 0.5 atm. The reaction products were analyzed by an on-line gas chromatograph with a 50-m Poraplot Q capillary column and a flame ionization detector (FID).

3. Results

The XRD patterns of the samples are shown in Fig. 1. It is evident that all the samples have a typical MFI structure [18]. The intensity of the diffraction peaks of S5 sample is a bit lower than the others, showing a slight decrease of crystallinity after desilication. With S3 as the reference, the crystallinity loss of S5 was calculated to be about 10% (see Table 1), suggesting that the framework structure of HZSM-5 was reasonably retained after alkaline treatment with aqueous solution of Na_2CO_3 and then acid treatment with HCl. The decrease in XRD crystallinity of S5 is most likely caused by the formation of framework defects through desilication, as demonstrated in ^{27}Al MAS NMR spectra presented in the following. The high relative crystallinity (97%) of the S6 sample indicates that use of starch as soft template for the generation of mesopores in HZSM-5 crystals is rather successful.

^{27}Al MAS NMR has been shown to be a powerful technique in the characterization of the local coordination environment of aluminum atoms in zeolites. It can discriminate between framework aluminum atoms in tetrahedral coordination and extra-framework aluminum atoms in octahedral coordination or penta-coordination (EFAL) [19–22]. ^{27}Al MAS NMR spectra of S3, S5 and S6 samples are

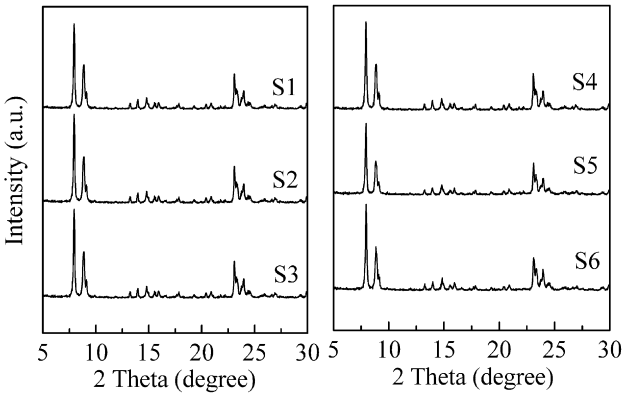

Fig. 1. XRD patterns of unmodified and mesopore-modified HZSM-5 zeolites.

Table 1
Physicochemical properties of the catalysts

Catalyst	Si/Al ratio[a]	S_{BET} ($m^2\ g^{-1}$)	V_{micro} ($cm^3\ g^{-1}$)	V_{meso} ($cm^3\ g^{-1}$)	B acid[b] (a.u.)	L acid[b] (a.u.)	Crystallinity (%)
S1	11	330	0.12	0.11	3.4	2.6	96
S2	42	329	0.12	0.10	2.3	2.2	100
S3	72	347	0.12	0.10	1.9	1.8	100
S4	114	339	0.12	0.10	1.1	1.2	100
S5	78	344	0.11	0.27	1.2	2.8	90
S6	76	367	0.11	0.47	1.4	1.7	97

[a] Si/Al molar ratio determined by ICP analysis.
[b] Brønsted and Lewis acidities were quantified according to the integrated areas of the absorbance peaks at 1540 and at 1450 cm^{-1}, respectively.

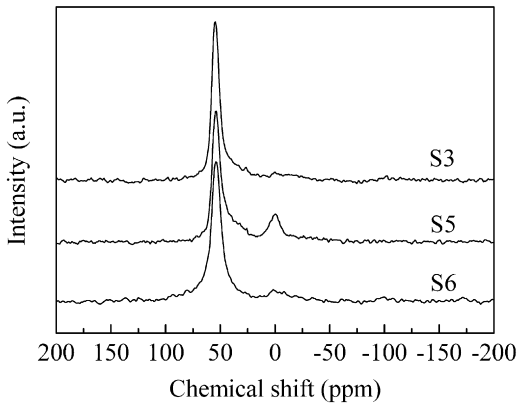

Fig. 2. ^{27}Al MAS NMR spectra of unmodified and mesopore-modified samples.

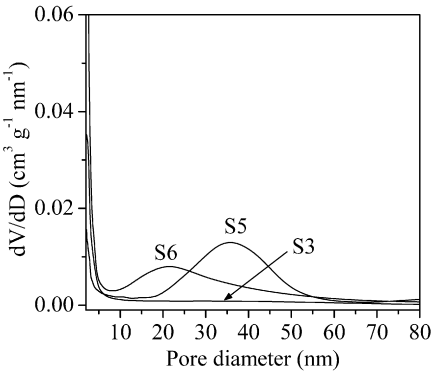

Fig. 3. Pore size distributions of unmodified and mesopore-modified samples.

shown in Fig. 2. The intense signal at 54 ppm is assigned to tetrahedrally coordinated framework aluminum in HZSM-5 zeolite, and the weak signal at 0 ppm can be attributed to octahedral extra-framework aluminum. There are almost no EFAL atoms in the S3 sample. A weak resonance at 0 ppm observed for the S5 sample suggests the existence of a small amount of EFAL atoms in this sample. This shows that the removal of framework Si in the zeolite upon alkaline treatment is probably accompanied by the cleavage of some Si–O–Al bonds, although the Si–O–Si bonds in the absence of neighboring Al ions are easier to hydrolyze and dissolve [23,24]. As a consequence, a small quantity of four-coordinated framework Al atoms are transformed into six-coordinated extra-framework ones in S5 sample after alkaline treatment. In the meantime, the number of EFAL atoms in S6 is significantly lower than that in S5. This is in agreement with the XRD crystallinity results.

The textural properties of the samples are listed in Table 1. The BET surface area of the untreated HZSM-5 (S3 sample) is 347 $m^2\,g^{-1}$. After the alkali-treatment there is almost no change in the BET surface area (344 $m^2\,g^{-1}$ for S5 sample). The S6 sample exhibits a somewhat larger surface area among all the samples. HZSM-5 zeolites with different Si/Al ratios in the 10–114 range (S1–S4 samples) exhibit mesopore volumes of ca. 0.10 $cm^3\,g^{-1}$, which are contributions from intercrystalline voids present between the nanophase crystalline particles [25]. After treatment of HZSM-5 in aqueous Na_2CO_3, the micropore volume decreases slightly from 0.12 to 0.11 $cm^3\,g^{-1}$, which is in agreement with the XRD results, whereas the mesopore volume increases significantly, i.e. from 0.10 to 0.27 $cm^3\,g^{-1}$. The pore size distribution curve in Fig. 3 demonstrates that the diameter of the newly created mesopores is in the range of 20–55 nm, centered around 35 nm. The significant increase in the mesoporosity of ZSM-5 zeolites upon alkaline treatment with aqueous NaOH was reported by several groups [13–17]. Our result is similar to the reported ones, although a milder and more controllable alkaline solution of Na_2CO_3 is used. An even larger mesopore volume of 0.47 $cm^3\,g^{-1}$ is observed for the S6 sample (Table 1), with diameter in the range of 10–50 nm, centered around 22 nm (Fig. 3).

Fig. 4 shows the surface morphology of representative samples. SEM images of S1, S2, S3 and S4 samples are similar. The particles of all the samples are sphere-like, and the distribution of the particle size seems to be rather uniform. The average particle size is ca. 500 nm in diameter for S1–S5 samples. The S6 sample exhibits a smaller average particle size of ca. 200 nm. The external surface of the as-synthesized HZSM-5 zeolites is clear and smooth. After treatment in alkaline media, the external zeolite surface becomes rough and rugged (Fig. 4b). It can be seen clearly that there are many nanoscale open holes on the exterior surface of S5. Furthermore, TEM image of the S5 sample (Fig. 5b) shows that the open holes are distributed on the surface without penetrating into

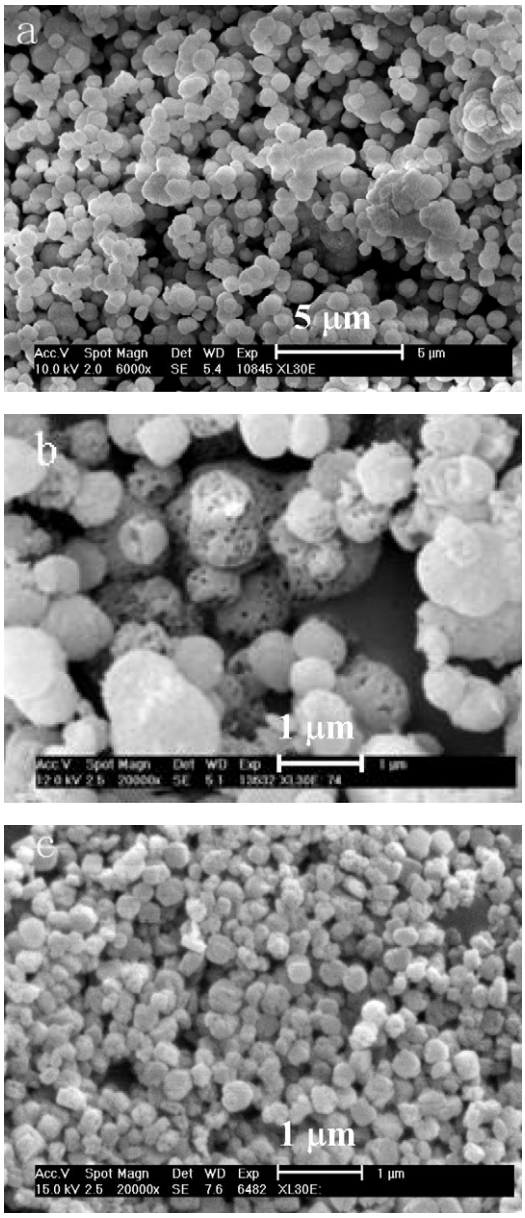

Fig. 4. SEM images of representative samples: (a) S3; (b) S5; (c) S6.

the crystals, i.e., the desilication takes place mainly on the surface and the interior of the zeolite crystals is almost unaffected upon alkaline treatment. The existence of these surface open holes is probably the main cause for the facilitation of molecular transport

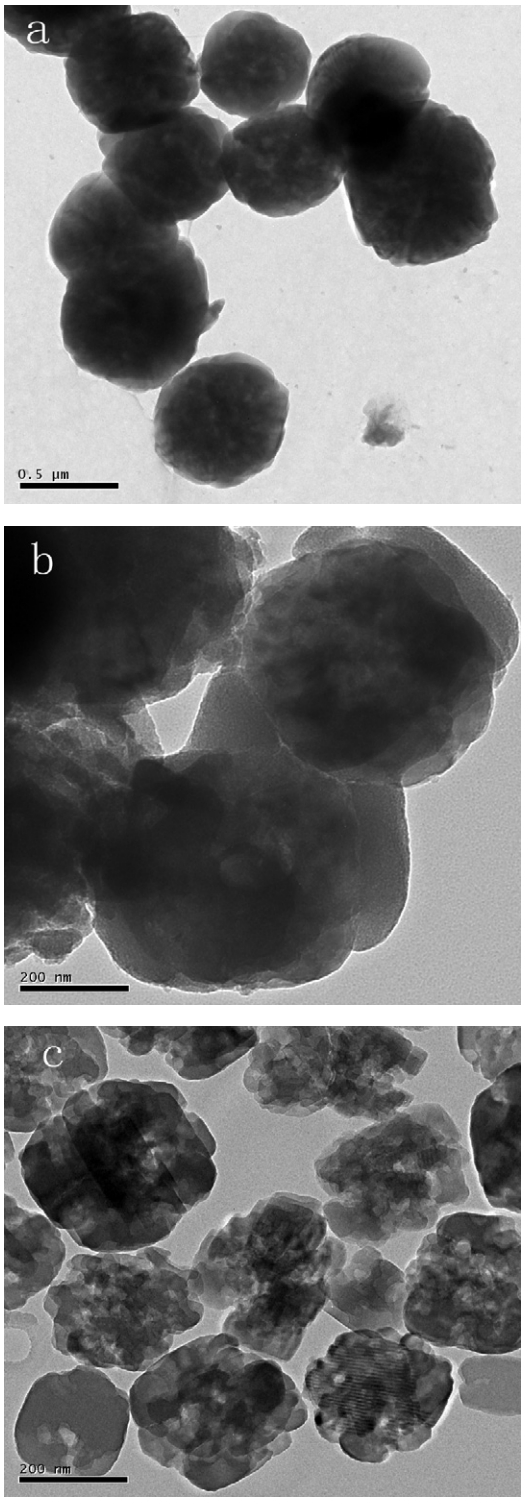

Fig. 5. TEM images of representative samples: (a) S3; (b) S5; (c) S6.

in MTP reaction and the improvement of catalytic performance of the HZSM-5 catalyst. In contrast, the outer surface of the crystals for the S6 sample is more or less smooth, as illustrated in Fig. 4c. However, there are many nanoscale mesopores randomly distributed in the bulk of the zeolite crystals, as evidenced by the TEM image (Fig. 5c). These mesopores are distributed inside the zeolite crystals and connected to the reaction system only through the narrow zeolite microporous channels. The morphological difference of these two types of mesopore-modified HZSM-5 catalysts

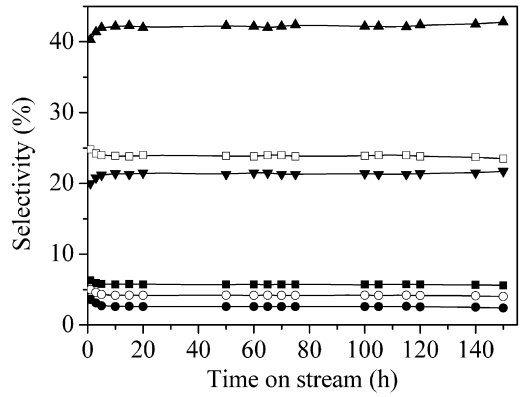

Fig. 6. Product selectivity of S5 as a representative catalyst for MTP reaction as a function of time: (▲) C_3H_6; (○) C_2H_4; (▼) C_4H_8; (●) aromatics; (■) C_1–C_4 saturated hydrocarbons; (□) C_5 and higher hydrocarbons excluding aromatics. Reaction conditions: $T = 470\,^{\circ}C$, WHSV $= 1\ h^{-1}$, $P_{CH_3OH} = 0.5$ atm, $H_2O{:}CH_3OH = 1{:}1$.

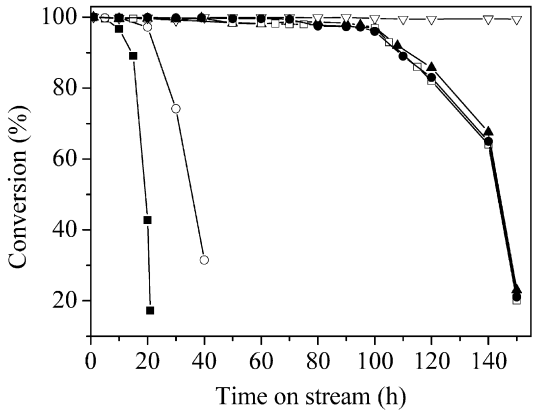

Fig. 7. Catalytic stability of unmodified and mesopore-modified HZSM-5 zeolites for MTP reaction: (■) S1; (○) S2; (▲) S3; (▽) S4; (□) S5; (●) S6. Reaction conditions: $T = 470\,^{\circ}C$, WHSV $= 1\ h^{-1}$, $P_{CH_3OH} = 0.5$ atm, $H_2O{:}CH_3OH = 1{:}1$.

is distinct, and its effect on the catalyst performance in MTP reaction is worthy to be further investigated.

Pyridine adsorption was followed by infrared spectroscopy to identify the number and nature of acid sites in the catalysts. FTIR spectra of the catalysts after pyridine adsorption at 200 °C and subsequent evacuation at 200 °C exhibit two characteristic bands at about 1540 and 1450 cm^{-1}, which are ascribed to pyridinium ions chemisorbed on Brønsted acid sites and coordinatively bound pyridine on Lewis acid sites, respectively [26–28]. Brønsted and Lewis acidities have been quantified according to the integrated areas of the peaks at 1540 and at 1445 cm^{-1}, respectively, and the data are summarized in Table 1. The number of Brønsted and Lewis acid sites present over S1–S4 catalysts follows the order of S1 > S2 > S3 > S4, as the same as that of the Si/Al ratio of these catalysts. A comparison of the acidity data for S3 and S5 demonstrates that alkaline treatment of the zeolite leads to a decrease in Brønsted acidity and an increase in Lewis acidity. This is due to the transformation of a part of four-coordinated framework Al atoms into six-coordinated extra-framework ones, as evidenced by ^{27}Al MAS NMR analysis (Fig. 2). The S6 catalyst has slightly more Brønsted acid sites and less Lewis acid sites, which is consistent with its higher relative crystallinity.

The changes in product selectivities with time on stream for S5 as a representative catalyst are presented in Fig. 6. At the initial stage the selectivities to propylene and butylene increase slightly, whereas the selectivities to ethylene, saturated hydrocarbons and aromatics decrease slightly. After 10 h on stream the reaction

Table 2
MTP reaction over unmodified and mesopore-modified HZSM-5 catalysts[c]

Catalyst	Conv. (%)	Selectivity (C-mol%)						P/E
		C_{1-4}[a]	C_2H_4	C_3H_6	C_4H_8	C_5^+[b]	Aromatics	
S1	99.6	20.5	15.3	26.7	4.25	16.6	16.7	1.75
S2	99.8	10.0	11.1	35.7	17.3	16.3	9.59	3.22
S3	99.6	9.55	10.1	37.0	20.5	17.1	5.75	3.66
S4	99.8	8.77	9.90	36.1	21.1	18.9	5.23	3.65
S5	99.6	5.72	4.18	42.2	21.4	23.9	2.60	10.1
S6	99.8	8.82	9.92	38.8	21.8	17.0	3.66	3.91

[a] C_1–C_4 saturated hydrocarbons.
[b] C_5 and higher hydrocarbons excluding aromatics.
[c] Reaction conditions: $T = 470\,^{\circ}C$, WHSV $= 1\ h^{-1}$, $P_{CH_3OH} = 0.5$ atm, H_2O: $CH_3OH = 1{:}1$.

reaches steady state. The methanol conversion over S5 catalyst drops obviously after on stream for 100 h, as shown in Fig. 7. However, the product selectivities are similar to those at steady state. The other catalysts display the same variation trend in product selectivities with time on stream. Table 2 shows the results of MTP reaction at steady state with water vapor as diluent gas on various HZSM-5 catalysts at 470 °C and atmospheric pressure. For the unmodified S1–S4 series catalysts, the propylene selectivity first increases and then decreases with an increase in Si/Al ratio. A maximum of 37.0% selectivity to propylene is achieved on S3 catalyst. The ethylene selectivity decreases gradually from 15.3 to 9.90%, as the Si/Al ratio is increased. As a result, the P/E ratio initially increases with Si/Al ratio and then levels off at a P/E ratio of ca. 3.7. In addition, the selectivity to aromatics decreases with increasing Si/Al ratio. Since S1–S4 series catalysts have similar particle sizes and textural properties, their difference in Brønsted acidity could be the main cause for the change in product distribution of the catalysts in MTP reaction. A decrease in Brønsted acidity of the catalysts favors the formation of propylene in the reaction and brings about an increase in P/E ratio from 1.75 to 3.66. However, as the Si/Al ratio increases to above 72, the effect of Brønsted acidity becomes less important. Meanwhile, the influence of mesopore-modification on product selectivity of the catalyst exceeds that of the acidity. For S5 catalyst, the propylene selectivity increases from 37.0 to 42.2% after modification, while the ethylene selectivity decreases from 10.1 to 4.18%, leading to a substantial increase of P/E ratio from 3.66 to 10.1. The increment of P/E ratio can be mainly attributed to the increase in mesoporosity of the HZSM-5 zeolite resulting from alkaline treatment, which facilitates the molecular transport in the MTP reaction exceedingly. It is noticed that the selectivity to propylene and P/E ratio are also improved on S6 catalyst. However, the improvement is obviously less striking than that on S5 catalyst. The probable reason is that the mesopores or cavities generated inside the zeolite crystals of S6 catalyst by using starch as soft template are not as efficient as the opened mesopores on the surface of S5 for the enhancement of diffusion of the gas molecules in the reaction process.

The catalytic stability of unmodified and mesopore-modified HZSM-5 zeolites for MTP reaction was tested at 470 °C, and the results are shown in Fig. 7. It can be seen that the catalytic stability of S1–S4 series catalysts follows the order of S4 > S3 > S2 > S1. Compared with S3 catalyst, the mesopore-modified catalysts (S5 and S6) exhibit similar stability. This indicates that base treatment does not improve the stability of the catalyst, although the propylene selectivity and P/E ratio are significantly increased. As shown in Fig. 7, the methanol conversion drops abruptly after on stream for some period. Coke deposition is the reason for catalyst deactivation [1]. When the coke accumulates to some amount, it would block the micropores of HZSM-5 and subsequently results in a sharp deactivation of the catalyst.

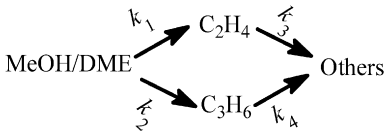

Scheme 1. The reaction pathway for methanol conversion.

4. Discussion

The catalytic conversion of methanol to olefins and hydrocarbons over acidic HZSM-5 zeolite consists of three categories of reactions: fast equilibrium of methanol (MeOH) with dimethyl ether (DME) over Brønsted acid sites, and thus MeOH and DME can be treated as a single kinetic species or lump [1,11,29,30]; the equilibrium mixture of MeOH and DME is then converted to the primary product of ethylene and propylene [1,31–33]; the subsequent conversion of the primary products into a mixture of higher olefins, paraffins and aromatics that can be lumped together (referred to as others) [1,32]. The simplified reaction pathway is shown in Scheme 1, where k_1 and k_2 are formation rate constants for ethylene and propylene respectively, and k_3 and k_4 are consumption constants for ethylene and propylene respectively.

The disappearance of oxygenates (mixture of MeOH and DME) and olefins (C_2H_4 and C_3H_6) is assumed to be first order [11, 32], then Eqs. (1), (2) and (3) are obtained, where k_{obs} is the rate constant of conversion of oxygenates. The parameter k_{obs} can be determined from conventional first-order semilog plots of oxygenates vs τ. If Eqs. (2) and (3) are divided by (1), Eqs. (4) and (5) are obtained after integrating, where $X_{MeOH/DME}$ is the conversion of oxygenates. A series of experimental data, i.e. $[C_2H_4]$, $[C_3H_6]$, [MeOH/DME] and $X_{MeOH/DME}$ can be acquired by changing the catalyst load, namely, the contact time. Fitting the experimental data using Eqs. (4) and (5) gives the values of $k_1 - k_4$.

$$-\frac{d[MeOH/DME]}{d\tau} = k_{obs}[MeOH/DME], \tag{1}$$

$$\frac{d[C_2H_4]}{d\tau} = k_1[MeOH/DME] - k_3[C_2H_4], \tag{2}$$

$$\frac{d[C_3H_6]}{d\tau} = k_2[MeOH/DME] - k_4[C_3H_6], \tag{3}$$

$$\frac{[C_2H_4]}{[MeOH/DME]} = \frac{k_1/k_{obs}[1-(1-X_{MeOH/DME})^{k_3/k_{obs}-1}]}{\frac{k_3}{k_{obs}}-1}, \tag{4}$$

$$\frac{[C_3H_6]}{[MeOH/DME]} = \frac{k_2/k_{obs}[1-(1-X_{MeOH/DME})^{k_4/k_{obs}-1}]}{\frac{k_4}{k_{obs}}-1}. \tag{5}$$

For kinetic measurements, the contact time in this work was changed in the range of 0.04 to 1.28 s. The formation and consumption rate constants of ethylene and propylene were calculated through fitting the experimental data with Eqs. (4) and (5). The effect of Si/Al ratio of HZSM-5 zeolite on the rate constants is shown in Fig. 8. As the Si/Al ratio increases, both k_1 and k_2 decline, but k_2 is always greater than k_1, indicating that propylene could be the dominant product on this type of catalysts. On the other hand, both k_3 and k_4 decrease with increasing Si/Al ratio, but k_4 drops much quicker than k_3, suggesting that the selectivity to propylene is more sensitive to the Brønsted acidity of the catalysts. Increasing the Si/Al ratio and reducing the Brønsted acidity of the catalysts, the consumption rate of propylene decreases more sharply than that of ethylene, hence the P/E ratio of the product is increased. However, the k_4 curve levels off at Si/Al ratio above 72, and the increase in selectivity to propylene and P/E ratio becomes insignificant. Therefore, adjusting the Si/Al ratio and Brønsted acidity of HZSM-5 catalysts can improve the product distribution in MTP reaction, but the amplitude of improvement is

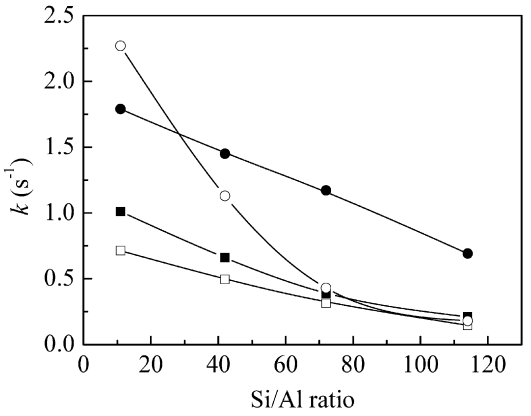

Fig. 8. Effect of Si/Al ratio of unmodified HZSM-5 zeolites on formation and consumption rate constants of propylene and ethylene: (■) k_1; (●) k_2; (□) k_3; (○) k_4.

limited due to reaction kinetic aspects. This explains that the maximum P/E ratio reached for the S1–S4 series catalysts in this work is less than 4.

The creation of mesopores in the zeolite crystals shortens the diffusion path of the primary olefin products and facilitates the removal of the olefins, in particular propylene and butylene with larger molecular sizes, from the reactive acid sites on the catalyst. As a result, the reaction equilibrium shifts to the formation of propylene and butylene, and also the probabilities that these olefins further form higher olefins, paraffins, aromatics and naphthenes via various secondary reactions on the acid sites of the catalysts are reduced. This leads to the increased selectivities to propylene, butylene and P/E ratio for S5 catalyst as compared with S3 catalyst (see Table 2). It is also interesting to note that different mesopore-modification methods of HZSM-5 zeolite catalyst may produce different aftereffects in MTP reaction. Besides the quantity of the mesopores created and the integrity of the zeolite crystals after treatment, a more important criterion of the modification is the openness of the mesopores. The mesopores in S6 catalyst created via the soft template route are randomly distributed in the zeolite particles and surrounded by the narrow microporous channels, so they are more diffusion limited than the open mesopores on the surface of S5 catalyst. This explains our experimental results that the improvement in selectivity to propylene and P/E ratio for S6 catalyst is not so evident as that for S5 catalyst. The lower selectivity to aromatics observed for S5 and S6 catalysts is a consequence of decreased probabilities for secondary reactions of propylene and butylene on the acid sites of the catalysts, because the creation of mesopores in the zeolite crystals facilitates the removal of these olefins. Although the soft template method is more simple and popular for mesopore development in practice, the present work proves that to create open mesopores in high silica HZSM-5 zeolite by alkaline treatment is probably a better way to fulfill the selectivity requirements in MTP reaction.

Recently, a hydrocarbon-pool mechanism has been suggested to explain the formation of light olefins for the MTO process under steady-state conditions on acidic zeolite catalysts [34–39]. According to this mechanism, polymethylbenzenes or their protonated counterparts, which are referred to as the hydrocarbon pool, serve as platforms to which methanol can bind and from which primary olefin products can dissociate. More recently, it has been shown that, besides the methylaromatics route, which is responsible for both ethylene and propylene formation, an additional olefins methylation/cracking route accounts for part of propylene formed on HZSM-5 zeolite catalyst. On the other hand, ethylene production is little influenced by the olefins route [40–42]. Based on this novel insight, in addition to improved diffusion, another cause for the increase in propylene selectivity upon the creation of mesopores in the zeolite crystals could be that the contribution of the olefins route to the propylene formation increases on the mesopore-modified HZSM-5 catalysts. The increased selectivity to C_5 and higher saturated hydrocarbons observed for S5 catalyst is an indirect evidence for improved contribution of the olefins route in MTP reaction over this catalyst, according to suggested dual cycle concept by Bjørgen and co-workers [42]. The lower ethylene selectivity observed for S5 catalyst may be a consequence of decreased contribution of the methylaromatics route in MTP reaction over this catalyst. In combination with higher propylene selectivity for S5 catalyst, higher P/E ratio was achieved on the high silica HZSM-5 catalyst modified by alkaline treatment.

5. Conclusions

Two kinds of mesopore-modified high silica HZSM-5 zeolites were prepared by alkaline treatment and soft template method. After alkali treatment, the structure of zeolite framework is scarcely damaged, and open holes with diameter of 20–55 nm are created on the zeolite crystal surface. These newly created open mesopores enhance the diffusion of the primary olefin products, in particular propylene and butylene, and inhibit undesirable secondary reactions. The propylene selectivity and P/E ratio of the HZSM-5 catalyst prepared by alkaline treatment reached 42.2% and 10.1, respectively. This P/E ratio is about thrice as large as that of ordinary high silica HZSM-5 catalyst. A large amount of mesopores with diameter of 10–50 nm are formed in HZSM-5 prepared by using starch as soft template. However, these mesopores locate inside the zeolite body and play a limited role in the diffusion of gas molecules, so the change in product selectivity for MTP reaction is insignificant on this type of modified HZSM-5 catalyst. The increase in propylene selectivity and P/E ratio upon the creation of mesopores in the zeolite crystals, especially by alkaline treatment, could be also due to different contributions of the methylaromatics route and olefins methylation/cracking route in MTP reaction on the modified and unmodified HZSM-5 catalysts. The present work demonstrates that the creation of open mesopore cavities or channels in HZSM-5 zeolite is as important as the right adjustment of its Brønsted acidity in the design and preparation of a good HZSM-5 catalyst for MTP reaction.

Acknowledgments

This work was financially supported by the Major State Basic Research Development Program of China (Grants 2003CB615801, 2003CB615802 and 2006CB806103).

References

[1] M. Stöcker, Microporous Mesoporous Mater. 29 (1999) 3.
[2] J.Q. Chen, A. Bozzano, B. Glover, T. Fuglerud, S. Kvisle, Catal. Today 106 (2005) 103.
[3] M. Hack, U. Koss, P. König, M. Rothaemel, H.D. Holtmann, US Patent 7 015 369 B2, 2006, to MG Technologies AG.
[4] F.A. Wunder, E.I. Leupold, Angew. Chem. Int. Ed. Engl. 19 (1980) 126.
[5] W.W. Kaeding, S.A. Butter, J. Catal. 61 (1980) 155.
[6] C.D. Chang, Catal. Rev. Sci. Eng. 26 (1984) 323.
[7] P.T. Barger, B.V. Vora, US Patent 6 534 692, 2003, to UOP LLC.
[8] T. Zhao, T. Takemoto, N. Tsubaki, Catal. Commun. 7 (2006) 647.
[9] T. Zhao, T. Takemoto, Y. Yoneyama, N. Tsubaki, Chem. Lett. 34 (2005) 970.
[10] S. Michael, S. Friedrich, B. Goetz, B. Henning, M. Friedrich-Wilhelm, Eur. Patent 0448000, 1991, to Sued Chemie AG and Metallgesellschaft AG.
[11] C.D. Chang, C.T.W. Chu, R.F. Socha, J. Catal. 86 (1984) 289.
[12] D. Prinz, L. Riekert, Appl. Catal. 37 (1988) 139.
[13] M. Ogura, S. Shinomiya, J. Tateno, Y. Nara, M. Nomura, E. Kikuchi, M. Matsukata, Appl. Catal. A 219 (2001) 33.
[14] L. Su, L. Liu, J. Zhuang, H. Wang, Y. Li, W. Shen, Y. Xu, X. Bao, Catal. Lett. 91 (2003) 155.

[15] J.C. Groen, L.A.A. Peffer, J.A. Moulijn, J. Pérez-Ramírez, Colloid Surf. A 241 (2004) 53.
[16] J.C. Groen, J.A. Moulijn, J. Pérez-Ramírez, Microporous Mesoporous Mater. 87 (2005) 153.
[17] Y. Tao, H. Kanoh, K. Kaneko, Adsorption 12 (2006) 309.
[18] R.J. Argauer, G.R. Landolt, US Patent 3 702 886, 1972, to Mobil Oil Corp.
[19] A.P. Kentgens, M.K. Scholl, W.S. Veeman, J. Phys. Chem. 87 (1983) 4357.
[20] J.B. Nagy, Z. Gabelica, G. Debras, E.G. Derouane, J.P. Gilson, Zeolites 4 (1984) 133.
[21] F. Deng, Y. Du, C. Ye, J. Wang, T. Ding, H. Li, J. Phys. Chem. 99 (1995) 15208.
[22] W. Liu, Y. Xu, S. Wong, J. Qiu, N. Yang, J. Mol. Catal. A 120 (1997) 257.
[23] T. Sano, Y. Nakajima, Z.B. Wang, Y. Kawakami, K. Soga, A. Iwasaki, Microporous Mater. 12 (1997) 71.
[24] J.C. Groen, L.A.A. Peffer, J.A. Moulijn, J. Pérez-Ramírez, Chem. Eur. J. 11 (2005) 4983.
[25] R. Ravishankar, C. Kirschhock, B.J. Schoeman, P. Vanoppen, P.J. Grobet, S. Storck, W.F. Maier, J.A. Martens, F.C. De Schryver, P.A. Jacobs, J. Phys. Chem. B 102 (1998) 2633.
[26] E.P. Parry, J. Catal. 2 (1963) 371.
[27] N.Y. Topsoe, K. Pedersen, E.G. Derouane, J. Catal. 70 (1981) 41.
[28] C.A. Emeis, J. Catal. 141 (1993) 347.
[29] J.R. Anderson, T. Mole, V. Christov, J. Catal. 61 (1980) 477.
[30] C.D. Chang, Chem. Eng. Sci. 35 (1980) 619.
[31] T.R. Forester, R.F. Howe, J. Am. Chem. Soc. 109 (1987) 5076.
[32] F.J. Keil, Microporous Mesoporous Mater. 29 (1999) 49.
[33] T.Y. Park, G.F. Froment, Ind. Eng. Chem. Res. 40 (2001) 4172.
[34] M. Seiler, W. Wang, A. Buchholz, M. Hunger, Catal. Lett. 88 (2003) 187.
[35] J.F. Haw, W. Song, D.M. Marcus, J.B. Nicholas, Acc. Chem. Res. 36 (2003) 317.
[36] M. Bjorgen, U. Olsbye, S. Svelle, S. Kolboe, Catal. Lett. 93 (2004) 37.
[37] U. Olsbye, M. Bjorgen, S. Svelle, K.P. Lillerud, S. Kolboe, Catal. Today 106 (2005) 108.
[38] J.F. Haw, D.M. Marcus, Top. Catal. 34 (2005) 41.
[39] W. Wang, Y. Jiang, M. Hunger, Catal. Today 113 (2006) 102.
[40] S. Svelle, F. Joensen, J. Nerlov, U. Olsbye, K.P. Lillerud, S. Kolboe, M. Bjørgen, J. Am. Chem. Soc. 128 (2006) 14770.
[41] S. Svelle, U. Olsbye, F. Joensen, M. Bjørgen, J. Phys. Chem. C 111 (2007) 17981.
[42] M. Bjørgen, S. Svelle, F. Joensen, J. Nerlov, S. Kolboe, F. Bonino, L. Palumbo, S. Bordiga, U. Olsbye, J. Catal. 249 (2007) 195.